Original Contribution

A diterpenoid derivate compound targets selenocysteine of thioredoxin reductases and induces Bax/Bak-independent apoptosis

Jinhua Liu [a], Chenglong Mu [a], Wen Yue [b], Jie Li [a], Biao Ma [a], Lixia Zhao [b], Lei Liu [b], Quan Chen [a,b], Chen Yan [c], Haiyang Liu [c], Xiaojiang Hao [c], Yushan Zhu [a,*]

[a] Tianjin Key Laboratory of Protein Science, College of Life Sciences, Nankai University, Tianjin 300071, China
[b] State Key Laboratory of Biomembrane and Membrane Biotechnology, Institute of Zoology, Chinese Academy of Sciences, Beijing 100101, China
[c] The State Key Laboratory of Phytochemistry and Plant Resources in West China, Kunming Institute of Botany, Chinese Academy of Sciences, Kunming 650204, China

ABSTRACT

We have previously shown that the natural diterpenoid derivative S3 induced Bim upregulation and apoptosis in a Bax/Bak-independent manner. However, the exact molecular target(s) of S3 and the mechanism controlling Bim upregulation are still not clear. Here, we identify that S3 targets the selenoproteins TrxR1 and TrxR2 at the selenocysteine residue of the reactive center of the enzymes and inhibits their antioxidant activities. Consequently, cellular ROS is elevated, leading to the activation of FOXO3a, which contributes to Bim upregulation in Bax/Bak-deficient cells. Moreover, S3 retards tumor growth in subcutaneous xenograft tumors by inhibiting TrxR activity *in vivo*. Our studies delineate the signaling pathway controlling Bim upregulation, which results in Bax/Bak-independent apoptosis and provide evidence that the compounds can act as anticancer agents based on mammalian TrxRs inhibition.

Crown Copyright © 2013 Published by Elsevier Inc. All rights reserved.

Introduction

Redox homeostasis is crucial for cellular viability and function [1–4], the balance of which is maintained by two major cellular antioxidant systems, the glutathione system and the thioredoxin (Trx) system [5]. The Trx system, which consists of thioredoxin, thioredoxin reductase (TrxR), and nicotinamide adenine dinucleotide phosphate (NADPH), plays important roles in antioxidant defense and redox-regulated signal transduction for cell growth and apoptosis [6–9]. Three TrxRs, cytosolic TrxR1, mitochondrial TrxR2, and testis-specific TrxR3, have been identified in mammalian cells [10–13]. TrxRs are essential mammalian selenoproteins that act as homodimers to catalyze NADPH-dependent reduction of Trx and other small molecular oxidants [14,15]. The fully oxidized enzyme accepts electrons from NADPH by reducing the bound flavin adenine dinucleotide (FAD) to flavin adenine dinucleotide reduced (FADH2), which passes the reducing equivalents to the N-terminal redox-active center in one subunit. This reduced N-terminal redox center transfers two electrons to the C-terminal redox-active selenocysteine (Sec) site in another subunit to generate the active enzyme [16–18]. The conserved Sec is essentially involved in the catalytic cycle of TrxR and is able to easily interact with its substrates and inhibitors according to the low pK_a (5.3) value of Selenol [16,17,19].

Both Trx and TrxR have important functions in the neoplastic growth of cancer cells and are key components of the resistant phenotype [20]. TrxR and components of Trx systems function as signaling factors that use critical cysteine motif(s) to act as redox-sensitive "sulfhydryl switches." These switches reversibly modulate specific signal transduction cascades, which regulate downstream proteins with similar redox-sensitive sites [21,22], and they are able to maintain critical cysteine residues present in transcription factors in a reduced state, which allows DNA binding. These transcription factors include nuclear transcription factor κ (NF-κB), the tumor suppressor p53 [23], the glucocorticoid receptor [24], hypoxia-inducible factor 1α (HIF-1α) [25,26], and the activator protein-1 (AP1) protein complex [21]. Both cytosolic and mitochondrial TrxR genes are essential for embryonic development, and knocked out these genes result in embryonic lethality [27–29]. Trx and TrxR have also been reported to be highly expressed in a

---

variety of cancers, including lung, colorectal, and pancreatic cancer [30–32], and increased expression of TrxR has been correlated with aggressive tumor growth, multiple drug resistance, poorer prognosis, and decreased patient survival [30,33]. Therefore, inhibition of TrxRs has been regarded as an important strategy for anticancer therapy [34,35]. This inhibition leads to p53-dependent cell cycle arrest or apoptosis [36] or Trx-dependent activation of apoptosis signal-regulating kinase 1 (ASK1) [37]. Alternatively, inhibition of TrxR hinders electron flux through the Trx system to change the redox conditions of cells, leading to the alteration of cellular signaling systems, and triggers apoptosis and necrosis due to reactive oxygen species (ROS) accumulation [38,39].

After exposing to apoptosis stress, the Bcl-2 family protein Bax and Bak induce the mitochondrial outer membrane permeabilization (MOMP) for the release of cytochrome c and lead the cells to undergo programmed cell death. Bax and Bak share a redundant function to initiate apoptosis in response to damaged cells or disorganized proliferation, especially in tumorigenesis [40,41]. However, in many kinds of tumors, the functions of Bax and Bak are downregulated through different ways. For example, Bax mutation has been identified in human leukemia, colorectal cancer, and gastrointestinal cancer [42,43]. Bak expression has also been abolished in skin cancer and gastric and colorectal cancers [44]. Therefore, innovative and specific approaches to overcome survival of the tumor cells in the absence of Bax and Bak function are urgently required. We previously found that natural diterpenoid derivative, 15-oxospiramilactone (hereafter named S3), induces Bax/Bak-independent apoptosis through the upregulation of a Bcl-2-interacting mediator of cell death (Bim), which interacts with Bcl-2 to permeabilize the mitochondrial outer membrane for cytochrome c release and apoptosis [45]. In an effort to understand the molecular targets of the compounds involved in the upregulation of Bim, we took a chemical biology approach and identified that S3 could target TrxR1 and TrxR2 and inhibited their antioxidant activities. Elucidation of the molecular signaling pathway controlling Bim upregulation by a small natural compound may hold promise for therapeutic applications of anticancer agents.

Materials and methods

Cell lines and reagents

SV40 T antigen-immortalized $bax^{-/-}/bak^{-/-}$ mouse embryonic fibroblast (MEF) cells and HCT116 $bax^{-/-}$ cells were maintained in Dulbecco's modified Eagle's medium (DMEM) medium supplemented with 10% fetal bovine serum (FBS) (Hyclone) and 1% penicillin–streptomycin at 37°C and 5% CO$_2$. Antibodies against the following proteins were used: β-actin (A5441, Sigma), TrxR1 (ab16840, abcam), c-Myc and TrxR2 (Sc-40, Sc-46279, Santa Cruz), Bim (C3405, CST), FOXO3a (2497, CST), p-FOXO3a (9465, CST), and Biotin (D5A7, CST). Commercial rat liver TrxR was purchased from Sigma (T9698). Other chemicals were purchased from Sigma unless otherwise specified.

TrxR1 and TrxR2 plasmid construction and protein purification

Full-length human TrxR1 (NM_001093771.2) and TrxR2 (NM_006440.3) and mouse TrxR1 (NM_001042513.1) and TrxR2 (NM_013711.3) cDNAs were amplified by PCR and cloned into the pcDNA4TO-myc vector. Mouse TrxR1 (Sec498A) and TrxR2 (Sec498A) site-directed mutant constructs were made using the site-directed mutagenesis kit. TrxR1 (Sec498C; Sec498A) and TrxR2 (Sec498C; Sec498A) were digested from the pcDNA4TO

vector with EcoRI and XhoI, and the fragments were then ligated into pGEX-4 T-1 vectors and expressed in *E. coli* BL21 cells. Protein expression was induced by adding 0.3 mM isopropyl β-D-1-thio-galactopyranoside (IPTG) and purified by glutathione-Sepharose columns (Roche). The purity of the proteins was assessed by SDS-PAGE followed by Coomassie brilliant blue (CBB) staining [46].

Detection of apoptotic activities

Cells were treated with 10 μM S3 or S1 (Fig. S1A and B) for the indicated time periods, and apoptosis was measured using the Annexin V detection kit according to the manufacturer's instructions. Flow cytometric analysis was performed to monitor the green fluorescence of FITC-conjugated Annexin V and the red fluorescence of DNA-bound propidium iodide (PI). All data were analyzed with Cell Quest software (BD).

Determination of TrxR activity in vivo and in vitro

For *in vivo* TrxR activity, $bax^{-/-}/bak^{-/-}$ MEFs were incubated with different concentrations (5, 10, and 20 μM) of S3 or S1 for 12 and 24 h. The control group contained the same amount of DMSO (1%, v/v). Next, the cells were washed with phosphate-buffered saline once and lysed with cell lysis buffer (0.5% NP-40, 150 mM NaCl, and 1 mM EDTA in TE buffer) with a protease inhibitor cocktail (Roche). The activity of TrxR in the cell extracts was determined as previously described [22].

For *in vitro* TrxR activity, commercial purified rat liver TrxR (Sigma) was first reduced by incubation with excess NADPH at room temperature for 5 min in buffer containing 50 mM Tris-Cl and 1 mM EDTA (pH 7.5). Next, appropriate amounts of S3 were added, followed by incubation at room temperature for the appropriate time. The control group contained the same amount of DMSO, and equal amounts of TrxR were subjected to the dithiobisnitrobenzoic acid (DTNB) assay as described above.

Binding kinetics of TrxR and Biotin–S3

Commercial rat liver TrxR1 (Sigma) was incubated with 40 μM Biotin–S3 for different time periods, and the covalently linked TrxR–Biotin–S3 complexes [TrxR–S3] were analyzed by SDS gel and subsequent Western blotting with anti-Biotin antibody. The protein bands on the gels were quantified by densitometry. Gel photographic images were processed using Image-J software.

The reaction rate constant of k_{obs} follows as the equations according to reference [47,48]:
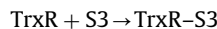
$$TrxR + S3 \rightarrow TrxR-S3$$

$$[TrxR]_t = [TrxR]_0 * E^{-kobs*t} \tag{1}$$

$$[TrxR-S3] = [TrxR]_0 - [TrxR]_t = [TrxR]_0 * (1 - E^{-kobs*t}), \tag{2}$$

where [TrxR–S3] is the complex of TrxR with S3, [TrxR]$_0$ is the total concentration, and [TrxR]$_t$ is TrxR concentration at time t.

Subcutaneous tumor implantation model

E1A/K-Ras-transformed $bax^{-/-}/bak^{-/-}$ MEFs and HCT116 $bax^{-/-}$ cells were harvested by centrifugation and suspended in PBS. A tumor cell suspension (5×10^5 $bax^{-/-}/bak^{-/-}$ MEFs or 3×10^6 HCT116 $bax^{-/-}$ cells in 100 μl PBS, respectively) was injected into the underarm of 4- to 5-week-old nude BALB/c mice, and then the mice were separated into three groups (6 mouse/group). Seven days after implantation, animals were intraperitoneally treated with S3 (30 mg/kg/day) or S1 (30 mg/kg/day) or vehicle control (50% (v/v) propylene glycol in 1.8% NaCl) every 3 days for 3 weeks.

All three groups of mice were sacrificed at the end of treatment and tumors were excised. The length (*a*) and width (*b*) of the tumor were measured using a slide gauge. Tumor sizes (*V*) were calculated according to the formula: $V = a*b^2/2$. Mice were maintained under specific pathogen-free (SPF) conditions, and all studies were approved by Animal Care and conformed to legal mandates and national guidelines.

ROS production determination

To detect ROS, growing (5×10^5 cells/ml) $bax^{-/-}/bak^{-/-}$ MEFs were incubated with S3 and S1 for the indicated times. Next, the cells were harvested, washed with PBS, and incubated with carboxy-2-7-dichlorodihydrofluorescein diacetate (H$_2$DCFDA) at 37 °C for 5 min. Green fluorescence intensity in the cells was examined by FACS (BD, USA) with excitation at 488 nm. PI (10 mg/ml) was added 1 min before flow cytometry. To validate the data, 0.1 mM H$_2$O$_2$ was added 0.5 h before staining (not shown). The data were analyzed with Cell Quest software (BD) using the cell population from which apoptotic cells were gated out against PI positivity.

Pull-down and mass spectrometric analysis of S3-bound proteins

$bax^{-/-}/bak^{-/-}$ MEFs were harvested and lysed in NP-40 lysis buffer, and then the cell lysates were incubated with Biotin or Biotin–S3 overnight at 4 °C. Proteins were bound to streptavidin agarose beads (Thermo) following the manufacturer's instructions. The beads were boiled with SDS loading buffer and subjected to SDS-PAGE and visualized by Coomassie brilliant blue (G250). The protein-containing bands in the gel were excised, followed by in-gel digestion and analysis by LC-MS/MS. Also, the proteins pulled down were confirmed by Western blotting with TrxR1 or TrxR2 antibody, respectively.

RNA interference

Pairs of complementary oligonucleotides against TrxR1 and TrxR2 were synthesized by Invitrogen (Shanghai), annealed, and inserted between the BamHI and HindIII sites of the pSilence2.1 hygro vector. The DNA sequence for mouse TrxR1shRNA was 5′-gatccgtcactttcaagctgtctaattcaagagattagacagcttgaaagtgagattttttg-gaaa-3′ and was 5′-gatccagcagagctttgatctcttctcaagagaaagagat-caaagctctgctgctttttttggaaa-3′ for TrxR2 shRNA. The resulting
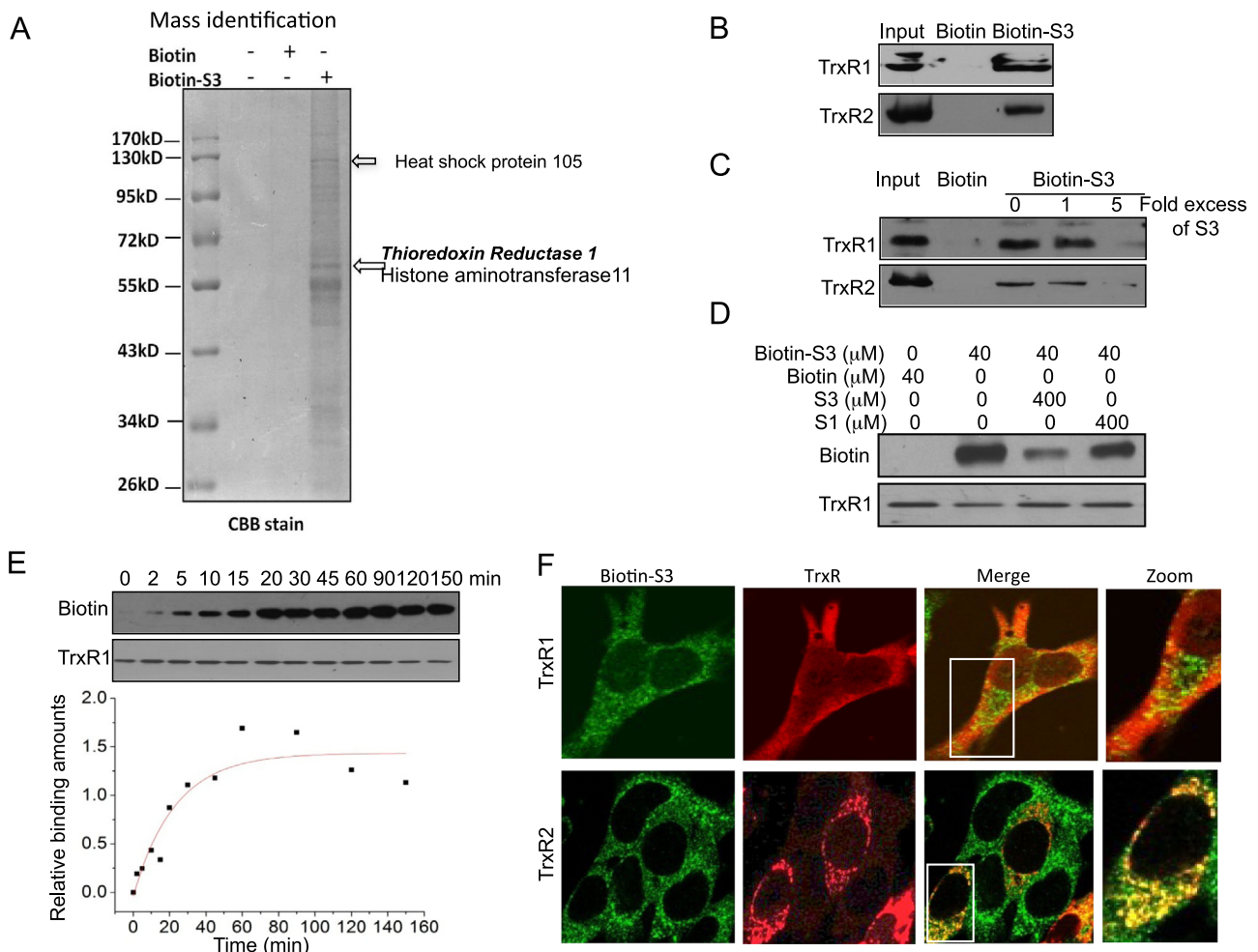

Fig. 1. S3 directly targets TrxR1 and TrxR2. (A) Biotin or Biotinylated-S3 was incubated with $bax^{-/-}/bak^{-/-}$ MEF cell lysates overnight at 4 °C, and then the streptavidin agarose was added into the lysates to isolate Biotinylated-S3 binding proteins. The eluted proteins were analyzed by SDS-PAGE and CBB staining. Bands of interest were cut, mass spectrometry analysis was performed, and TrxR proteins were detected by Western blotting as indicated in B. (C) $bax^{-/-}/bak^{-/-}$ MEF cell lysates were incubated with Biotin–S3 or Biotin in the absence or presence of a 1- or 5-fold excess of unlabeled S3, followed by pull-down with streptavidin-agarose. The precipitates were resolved by SDS-PAGE and detected by Western blotting for TrxR1 or TrxR2 antibody as indicated. (D) Recombinant mouse liver TrxR protein was incubated with Biotin–S3 in the absence or presence of a 10-fold excess of unlabeled S3 or S1 for 30 min, and SDS-PAGE analyzed by anti-TrxR1 or anti-Biotin antibody, respectively. (E) The determination of interaction of TrxR with Biotin–S3 at different times as described under Materials and methods. (F) Confocal microscopy images of the $bax^{-/-}/bak^{-/-}$ MEFs that were treated with 10 μM Biotin–S3 for 2 h and stained with anti-Biotin, anti-myc primary antibody, and Cy3- or FITC-conjugated secondary antibodies. The data are representative of three independent experiments.

plasmids (1.5 μg) were individually transfected into $bax^{-/-}/bak^{-/-}$ MEFs using polyethyleneimine (PEI). Transfectants were selected in culture medium containing 100 μg/ml hygromycin.

Double TrxR1/TrxR2 knocked down cells were acquired by transfection of the TrxR2 siRNA into the stable knocked down TrxR1 by shRNA.

Immunofluorescence assay

$Bax^{-/-}/bak^{-/-}$ MEFs transfected with myc-TrxR1 or myc-TrxR2 grown on coverslips were treated with 10 μM Biotin–S3 for 2 h and washed with phosphate-buffered saline (PBS) and fixed in 4% formaldehyde in DMEM for 30 min at 37 °C. Fixed cells were permeabilized with 0.2% Triton X-100 in PBS for 5 min on ice and blocked with 3% BSA in PBS for 1 h. Next, the cells were stained with primary antibodies (anti-Myc, anti-Biotin) overnight at 4 °C followed by incubation with fluorescent conjugated secondary antibodies. Unbound antibody was removed with PBS, and the cells were imaged using a Zeiss fluorescence microscope.

Statistical analysis

Data are expressed as mean ± standard error of the mean (SEM). Significant differences between values under different experimental conditions were determined using the paired or unpaired Student t test with repeated measurements, and $P < 0.05$ was considered statistically significant.

Results

S3 directly targets TrxR1 and TrxR2

In our previous study, we found that the natural diterpenoid derivative S3 could induce apoptosis in Bax/Bak double knockout MEFs ($bax^{-/-}/bak^{-/-}$) and upregulated Bim expression [45]. All of these observations prompted us to identify the potential targets of S3 that are responsible for its apoptosis inducing action. For this purpose, synthetic derivatives of natural products have been shown to be useful chemical probes. Thus, Biotin-tagged S3 (hereafter named Biotin–S3) was synthesized on the basis of a structure–activity relationship. Next, Biotin–S3 and free Biotin were incubated with $bax^{-/-}/bak^{-/-}$ MEFs cell lysates, and the bound proteins were precipitated with streptavidin-coated agarose beads, followed by gel electrophoresis and mass spectrometric analysis. The results identify that one of the bands at 55 kDa contains TrxR1 (Fig. 1A), which is selenoprotein that localizes in cytoplasm and has high homology with mitochondrial TrxR2.
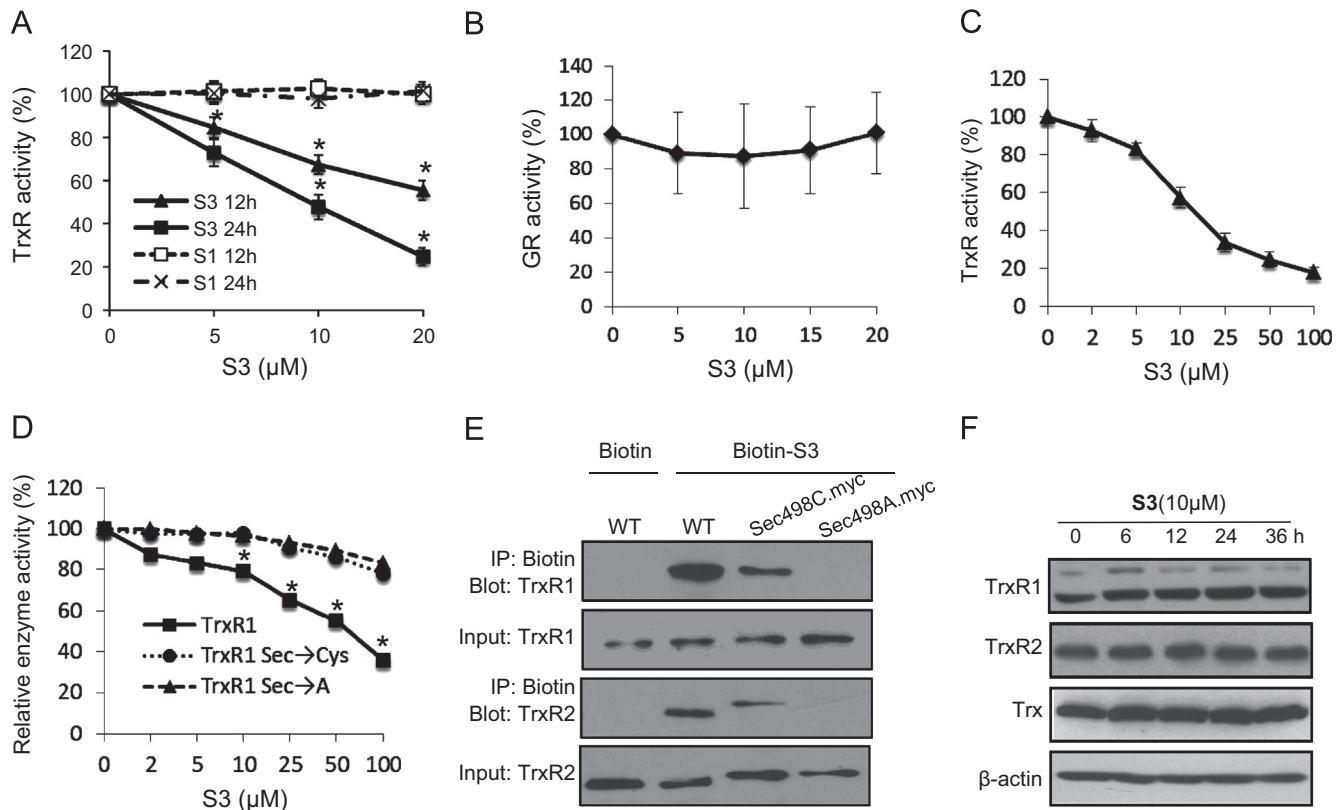

Fig. 2. S3 attenuates TrxR activity by specifically binding the selenocysteine site. (A) $bax^{-/-}/bak^{-/-}$ MEFs were treated with the indicated concentration of S3 or S1 for 12 and 24 h and then collected, followed by preparation of cell lysates with a protease inhibitor cocktail. Equal amounts of total cellular protein (5 μg) were added to the reaction system to determine the activity of total TrxR. (B) $bax^{-/-}/bak^{-/-}$ MEFs were treated with the indicated concentration of S3 for 24 h, collected, and lysed in the NP-40 lysis buffer with a protease inhibitor cocktail. GR activity was measured by the GSSG reduction assay. (C) Commercial rat liver TrxR1 was first reduced by incubation with NADPH at room temperature for 5 min in a buffer containing 50 mM Tris-Cl and 1 mM EDTA and incubated with S3 at different concentrations, and then TrxR activity was determined using the DTNB reduction assay. (D) Commercial rat liver TrxR1 and recombinant TrxR1 mutants (Sec498Cys) and (Sec498A) protein were prereduced by NADPH for 5 min and incubated with the indicated concentrations of S3 for 30 min. The relative activity of the TrxR 1 was detected using the DTNB reduction assay. (E) TrxR1 and TrxR2 KD cells were transfected with wild-type TrxR1/2 (full CDS with 3′-stem loop and no tag), TrxR1/2(Sec498Cys), and (Sec498A) (full CDS with myc tag). The cell lysates were then incubated with Biotin and Biotin–S3 overnight at 4 °C and modified proteins were bound to streptavidin agarose beads followed by blotting with Biotin and TrxR1/2. (F) $bax^{-/-}/bak^{-/-}$ MEFs were treated with 10 μM S3 for the indicated times. Cell lysates were collected, and equal protein contents were analyzed by Western blotting with the indicated antibodies. β-Actin was used as the control. The data are representative of the mean value of at least three separate experiments, and statistical significance was determined by Student's t test, $^{*}P < 0.05$ compared with the untreated group.

Thus, we further blotted the precipitates with antibodies against TrxR1, TrxR2. As shown in Fig. 1B, $bax^{-/-}/bak^{-/-}$ MEF cells expressed two TrxR isoforms (TrxR1, TrxR2), and Biotin–S3 effectively pulled down these proteins (Fig. 1B). The binding was competed away by high concentrations of unlabeled S3, indicating that the protein that bound Biotin–S3 also bound S3 (Fig. 1C). Biotin–S3 also effectively bound commercial rat liver TrxR1 in vitro, and this binding was competitively inhibited by higher concentrations of unlabeled S3 (Fig. 1D). S1, an analogue (supplementary Fig. 1) that fails to induce Bim upregulation and apoptosis, does not block Biotin–S3 binding to TrxR1 (Fig. 1D). Next, we detected the binding kinetic characteristics between TrxR1 and Biotin–S3 at indicated times, and the results showed a time-dependent manner that is consistent with an irreversible mechanism of binding [49]. Furthermore, the rate constant for binding (K_{obs}) was calculated to be approximately 0.0302 according to the formula used, indicating a high affinity for their interaction (Fig. 1E). Immunofluorescence staining results also demonstrated that Biotin–S3 is cell permeable and is present in the cytoplasm with TrxR1, and it was slightly enriched in mitochondria where TrxR2 is expressed in $bax^{-/-}/bak^{-/-}$ MEFs (Fig. 1F, supplementary Fig. 2). Collectively, these results revealed that TrxR1 and TrxR2 are potential targets of S3.

S3 targets the selenocysteine of TrxR and inhibits its catalytic activity

To understand the biological significance of the interaction between S3 and TrxR1/2, we examined whether S3 inhibits TrxR activity in $bax^{-/-}/bak^{-/-}$ MEFs. After treatment of $bax^{-/-}/bak^{-/-}$ MEFs with S3 at the indicated concentration for 12 and 24 h, TrxR activity was significantly reduced, while S1 had no such effect (Fig. 2A). The IC_{50} value of S3 was approximately 6.0 μM for 24 h (Fig. 2A). We also examined whether S3 also inhibited the activity of glutathione reductases (GRs), which are structurally and mechanistically related to TrxR but do not have Sec in the reactive center. We found that TrxR, but not GR, was efficiently inhibited by S3 (Fig. 2B). To further confirm the specific inhibitory effects of S3 on TrxR, we next examined the inhibitory effect of S3 on commercial TrxR1 from rat liver in vitro and found that S3 but not S1 inhibited TrxR activity in a time- and dose-dependent manner (Fig. 2C, supplementary Fig. 3). These results demonstrated that S3 could specifically inhibit TrxR activity in vivo and in vitro.

S3 has a α,β-unsaturated ketone at C15 position which was called "Michael reaction acceptor," while there is a hydroxyl group at the same position for S1, thus S3 has far more reactivity with selenyl than S1. This prompted us to investigate whether S3 may directly interact with the Sec site of TrxR. Mammalian TrxR1
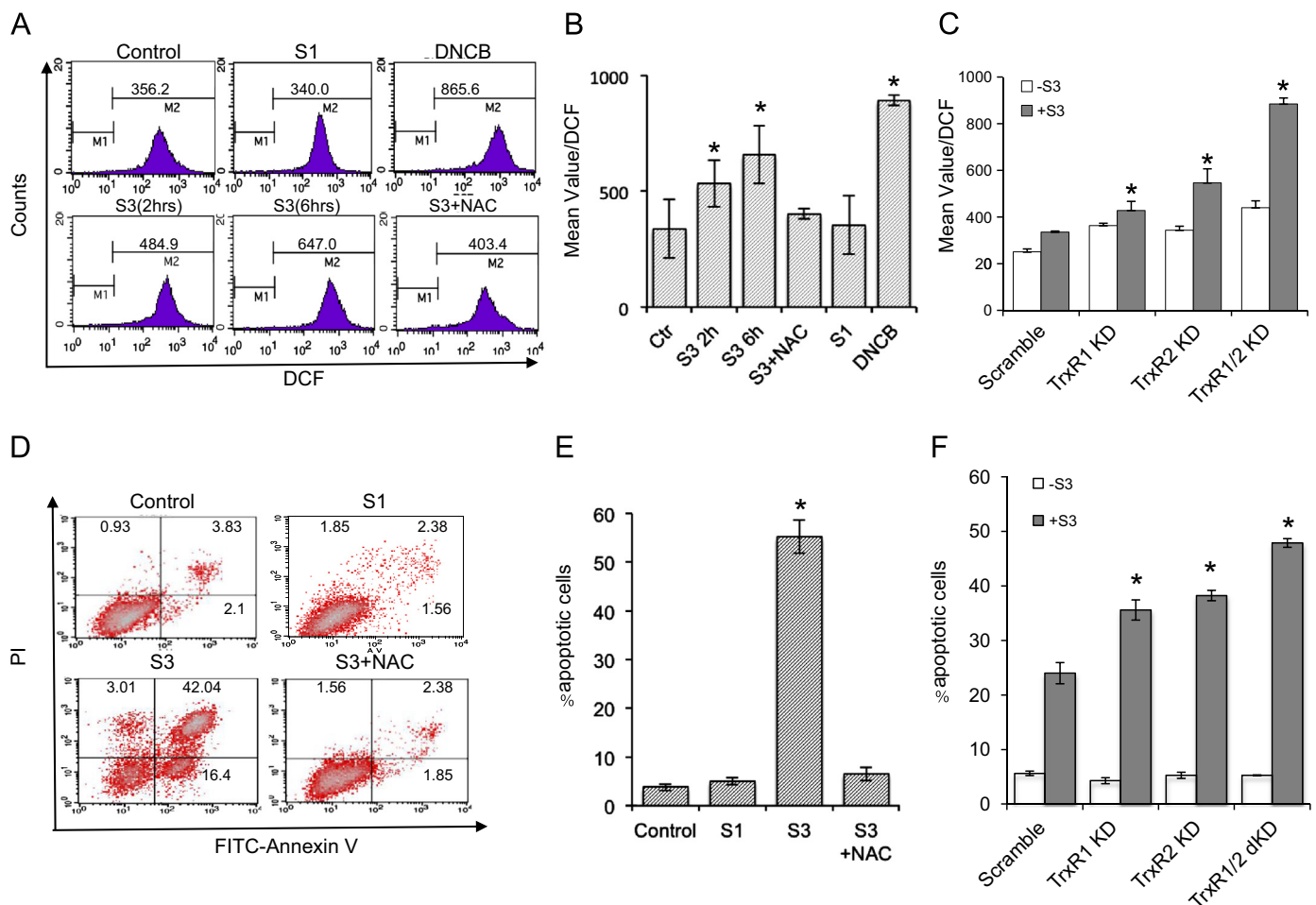

Fig. 3. S3 induces oxidative stress-dependent cell death. (A) $bax^{-/-}/bak^{-/-}$ MEFs were treated with S3, S1, or DNCB at the indicated times, the cells were then washed with PBS and stained with CM-H2DCF-DA for 5 min, and the cells were immediately analyzed using flow cytometry; the statistical results of the ROS levels are indicated in B. (C) Flow cytometry analysis of the ROS levels in TrxR1, TrxR2, and TrxR1/2 knock down $bax^{-/-}/bak^{-/-}$ MEFs that were treated with or without S3 for 2 h. (D and E) $bax^{-/-}/bak^{-/-}$ MEFs were pretreated with or without NAC for 30 min and then incubated with 10 μM S3 for another 48 h. The percentage of apoptotic cells was characterized with Annexin V (AV); statistical results of the apoptotic level are indicted in E. (F) Flow cytometric analysis of the apoptosis in TrxR1, TrxR2, and TrxR1/2 knock down $bax^{-/-}/bak^{-/-}$ MEFs that were treated with or without S3 for 24 h. The data are the representative of the mean value of at least three separate experiments, and statistical significance was determined using Student's t test. $^*P < 0.05$ compared with the control group.

has two redox-active sites; one is located at the N-terminus (Cys59/Cys64) and the other at the C-terminus (Cys497/Sec498) [16,19]. Therefore, in principle, blocking either the N-terminal or the C-terminal active site could lead to inactivation of the enzyme. We studied the inhibitory properties of S3 on two mouse TrxR1 (mTrxR1) mutants in comparison to wild-type TrxR1 to characterize the inhibitory specificity of S3 and to determine its target site. We designed two mTrxR1 mutant recombinant enzymes -TrxR1 (Sec498Cys) and TrxR1 (Sec498A). In the case of the mTrxR1 Sec498 Cys mutant, only very high concentrations of S3 (about 100 μM incubated for 30 min) inhibited the DTNB reduction activity of this protein. This indicated that the mTrxR1 (Sec498Cys) mutant was much less sensitive to S3 compared to the wild-type mTrxR1 (Fig. 2D) and implied that the Sec residue is important for the inhibitory mechanism of S3 on mammalian wild-type TrxR1. The TrxR1 (Sec498A) mutant lacks C-terminal catalytic activity but can reduce DTNB via the intact N-terminal active site [50], proving that the N-terminal active site is not involved in the inhibitory mechanism of S3 on TrxR1 (Fig. 2D). Pull-down assay further revealed that only wild-type TrxR has the strongest interaction with Biotin–S3 compared to the TrxR1 (Sec498Cys) mutant; however, TrxR1 (Sec498A) failed to interact with S3 (Fig. 2E). Similar results were found with TrxR2 (Fig. 2E). To exclude the possibility that S3 may downregulate the expression level of TrxR, we also checked the expression level of TrxR and Trx in $bax^{-/-}/bak^{-/-}$ MEFs. Western blot results showed that the protein levels of TrxR1, TrxR2, and Trx had no apparent change before and after S3 treatment (Fig. 2F). Taken together, these results suggest that S3 specifically targets the C-terminal redox-active site of mammalian TrxR1 and TrxR2 at 498 s residues to inhibit their activities.

S3 induces oxidative stress-dependent cell death

The TrxR/Trx system plays a critical role in the defense against oxidative stress [19,30,51]. Since S3 inhibits the activity of TrxRs, it is therefore of interest to study whether S3 increases the level of ROS in $bax^{-/-}/bak^{-/-}$ MEFs. As shown in Fig. 3A and B, ROS levels significantly increased at 6 h after S3 treatment compared with untreated cells. Pretreatment with N-acetyl-L-cysteine (NAC) effectively blocked S3-induced ROS accumulation. Also, S3-induced apoptosis was significantly blocked by NAC (Fig. 3D and E), suggesting that the induction of ROS is linked to apoptosis. Similar apoptosis results were obtained when HCT116 $Bax^{-/-}$ were used (Supplementary Fig. 6). The 3-(4,5-dimethylthiazol-2-yl)-2,5-diphenyltetrazolium bromide (MTT) assay also showed that S3 inhibited the cell proliferation of $bax^{-/-}/bak^{-/-}$ MEFs in a dose- and time-dependent manner (supplementary Fig. 4).

To further elucidate the role of TrxR in S3-induced ROS production and apoptosis, we used shRNA to specifically knock down TrxR1 and TrxR2 expression simultaneously or independently by 60–80% in $bax^{-/-}/bak^{-/-}$ MEFs (Fig. S5). We found that cell death and ROS production both increased when TrxR1 or TrxR2 were knocked down compared with the scramble cells. Knockdown of both TrxR1 and TrxR2 further increased the sensitivity to S3 treatments (Fig. 3C and F). Taken together, these results showed that S3 attenuates TrxR activity and increases ROS production to promote apoptosis.

TrxRs mediate Bim upregulation via the accumulation of ROS

Next, we addressed the issue of whether ROS generation caused by TrxR inhibition results in the upregulation of Bim
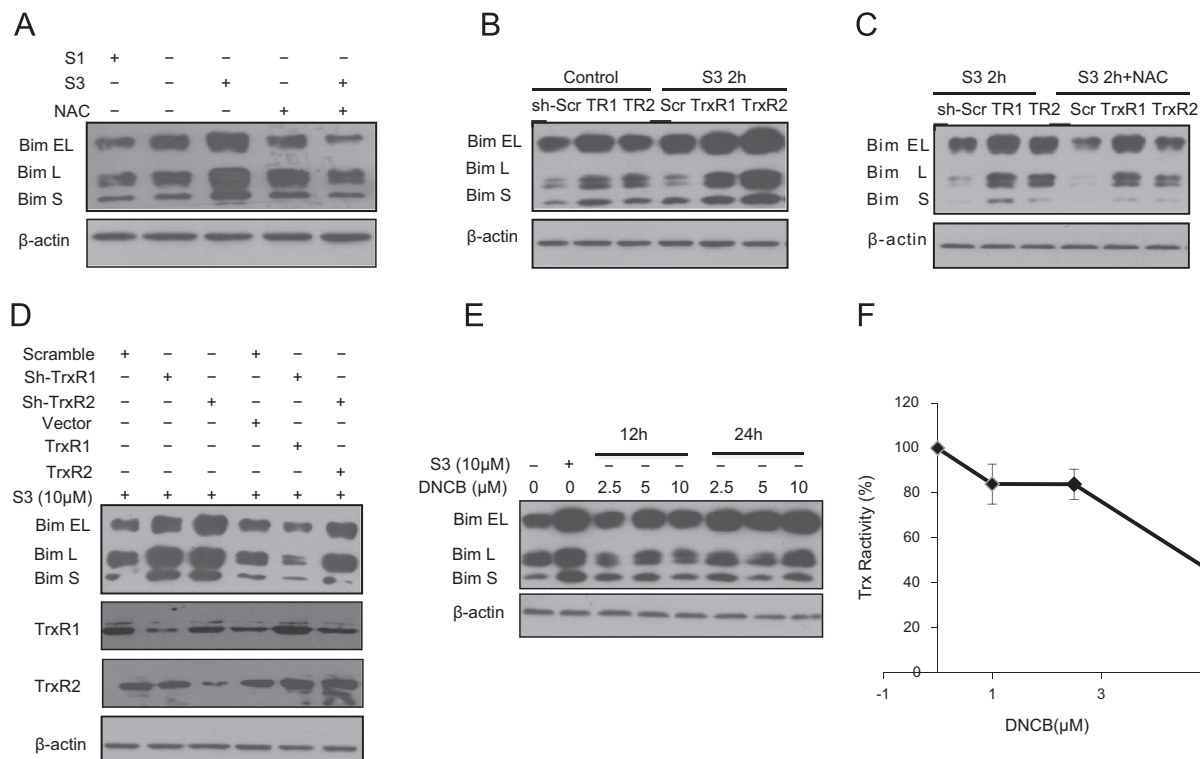

Fig. 4. TrxRs mediate Bim upregulation via the accumulation of ROS. (A) Immunoblotting of $bax^{-/-}/bak^{-/-}$ MEFs treated by S3 and S1 after pretreatment with or without 10 mM NAC for 30 min, with specific antibody for Bim, displaying its three isoforms: Bim EL(~25 kDa), Bim L(~18 kDa), and Bim (~15 kDa). (B) The scramble, TrxR1 KD, and TrxR2 KD cells were treated with or without S3 for 2 h and then Western blotting analysis of Bim expression was performed. (C) The scramble, TrxR1 KD, and TrxR2 KD cells were pretreated with or without NAC followed by S3 treatment for 2 h, and Bim expression was then analyzed by Western blotting. (D) The scramble,TrxR1, and TrxR2 KD cells were introduced into the ectopic expression of control vector, RNAi resistant TrxR1 or TrxR2 (full CDS with 3′-stem loop), respectively, and treated with 10 μM S3; then Bim expression was detected. (E and F) $bax^{-/-}/bak^{-/-}$ MEFs were treated with the indicated concentration of DNCB for 12 h, TrxR activity was analyzed using DTNB assay (F), and Bim expression was then analyzed by Western blotting (E).
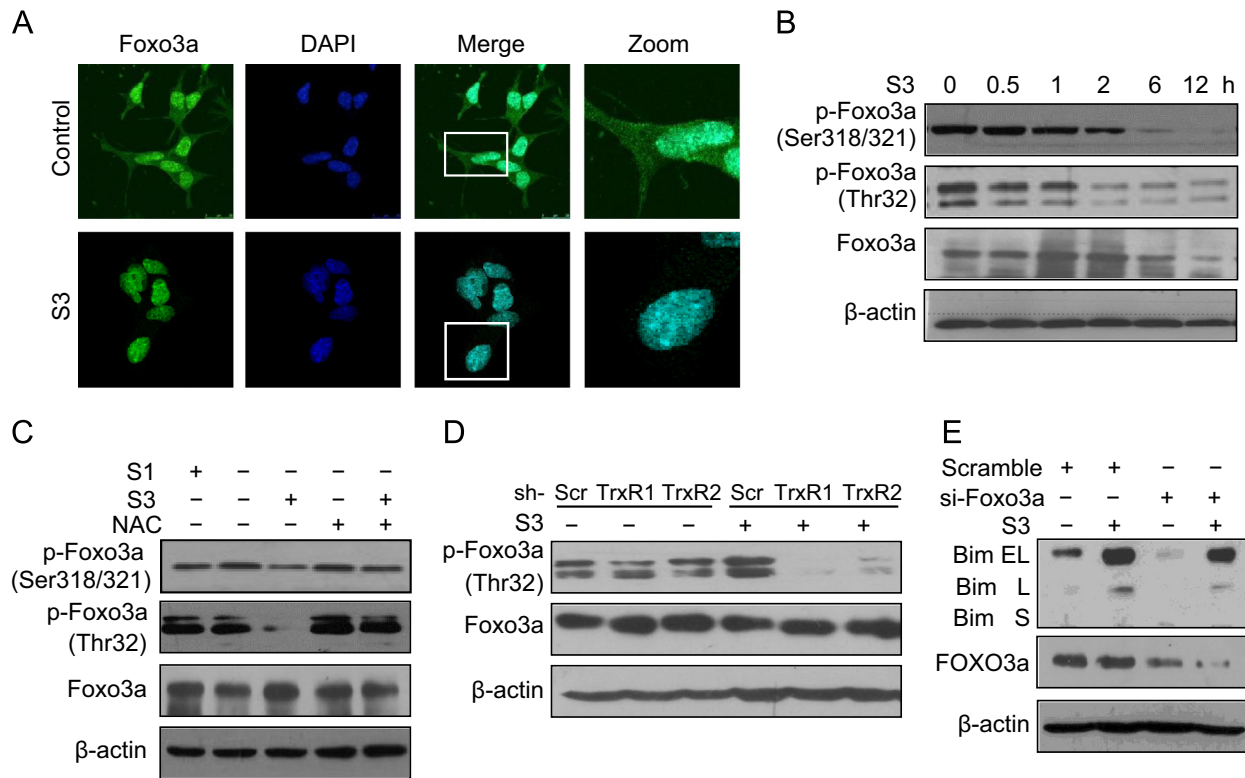
Fig. 5. S3 induces nuclear translocation and FOXO3a activation. (A) Confocal microscopy images of $bax^{-/-}/bak^{-/-}$ MEFs treated with 10 μM Biotin–S3 for 2 h and stained with anti-FOXO3a followed by incubation with the FITC-conjugated secondary antibody and DAPI. (B) $bax^{-/-}/bak^{-/-}$ MEFs were treated with 10 μM S3 for the indicated times, and Western blotting detected the p-FOXO3a (Ser318/321), p-FOXO3a (Thr32), and total FOXO3a levels using the specific antibody. (C) $bax^{-/-}/bak^{-/-}$ MEFs were pretreated with or without NAC for 30 min, followed by incubation with 10 μM S3 or 10 μM S1 for another 12 h. Western blotting analyzed the protein levels of p-FOXO3a (Ser318/321), p-FOXO3a (Thr32), and FOXO3a. (D) Western blotting analysis of p-FOXO3a (Thr32) and FOXO3a in the $bax^{-/-}/bak^{-/}$ cells that knocked down TrxR1 or TrxR2 expression with or without 10 μM S3 treatment for 2 h. (E) Western blotting analysis of Bim expression in $bax^{-/-}/bak^{-/-}$ MEFs that knocked down FOXO3a expression by siRNA after with or without 10 μM S3 treatment for 12 h.

expression in $bax^{-/-}/bak^{-/-}$ MEFs following S3 treatment. First, we showed that pretreatment with NAC blocked the upregulation of Bim (Fig. 4A). Also, knocked down the expression of TrxR1 or TrxR2 resulted in the upregulation of Bim, which was further enhanced by S3 treatment (Fig. 4B) and was blocked by NAC (Fig. 4C). A rescue experiment involving the reintroduction of wild-type TrxR1 or TrxR2 into TrxR knockdown cells further demonstrated that TrxRs were responsible for Bim upregulation (Fig. 4D). To determine if the increased expression of Bim by S3 is common to TrxR inhibitors, we investigated the effect of a well known TrxR inhibitor dinitrochlorobenzene (DNCB) [52]. $bax^{-/-}/bak^{-/-}$ MEFs exposed to DNCB displayed a dose-dependent inhibition of TrxR and a concomitant increase in Bim expression (Fig. 4E and F). Therefore, we concluded that inhibition of TrxR resulted in ROS production and Bim upregulation.

S3 induces the activation of FOXO3a and its nuclear translocation

Previous studies have shown that FOXO3 translocates from the cytosol to the nucleus and acts as a transcription factor that regulates Bim expression in response to oxidative stress [53–55]. We also found that FOXO3a is located in both the cytoplasm and the nucleus in untreated $bax^{-/-}/bak^{-/-}$ MEFs, but it was detected predominantly in the nucleus following S3 treatment (Fig. 5A). Western blotting analysis showed that S3 but not S1 caused activation of FOXO3a, as indicated by the dephosphorylation of Thr32 and Ser 318/321, while the protein levels of FOXO3 have no apparent change (Fig. 5B and C). The activation of FOXO3 can be prevented by pretreatment with NAC (Fig. 5B and C). Furthermore, we found that dephosphorylation of FOXO3a on Thr-32 was enhanced after S3 treatment in TrxR1 or TrxR2 knockdown

$bax^{-/-}/bak^{-/-}$ MEFs compared to scramble cells (Fig. 5D). To ascertain that FOXO3a is responsible for Bim upregulation in $bax^{-/-}/bak^{-/-}$ MEFs following S3 treatment, we knocked down FOXO3a and found that Bim expression is markedly reduced in the presence of S3 (Fig. 5E). Taken together, our results suggest that the inhibition of TrxR1 and TrxR2 by S3 is responsible for ROS production, which activates FOXO3a leading to the upregulation of Bim expression.

S3 retards tumor growth through the inhibition of TrxR

We next determined if the inhibition of TrxR activity by S3 is correlated with tumor growth retardation of $bax^{-/-}/bak^{-/-}$ MEFs using a xenograft model. Immortalized $bax^{-/-}/bak^{-/-}$ MEFs [45,56] were injected into nude mice and then treated with S3, S1, or vehicle control. S3 but not S1 or vehicle alone significantly reduced the size and weight of the tumors compared to the controls (Fig. 6A–C). No weight loss was observed when treated with S3 compared with the vehicle group (Fig. 6F). Similar results were obtained for the implanted HCT116 $bax^{-/-}$ colon cancer cells (supplementary Fig. 7). TUNEL assay showed an increase of apoptotic cells in tumors from the group treated with S3 compared with those from the control group (just as we previously reported). TrxR activity was significantly reduced in these tumors by S3 treatment compared with the control (Fig. 6D). However, liver TrxR activity did not change (Fig. 6E), which may be due to the higher absorption of the compound in tumors and differing metabolic activities between the tumors and the liver. Furthermore, Western blotting analysis found the upregulation of Bim expression in tumors (Fig. 6G) but not liver tissues (data not shown) with treatment with S3. These results indicate that S3
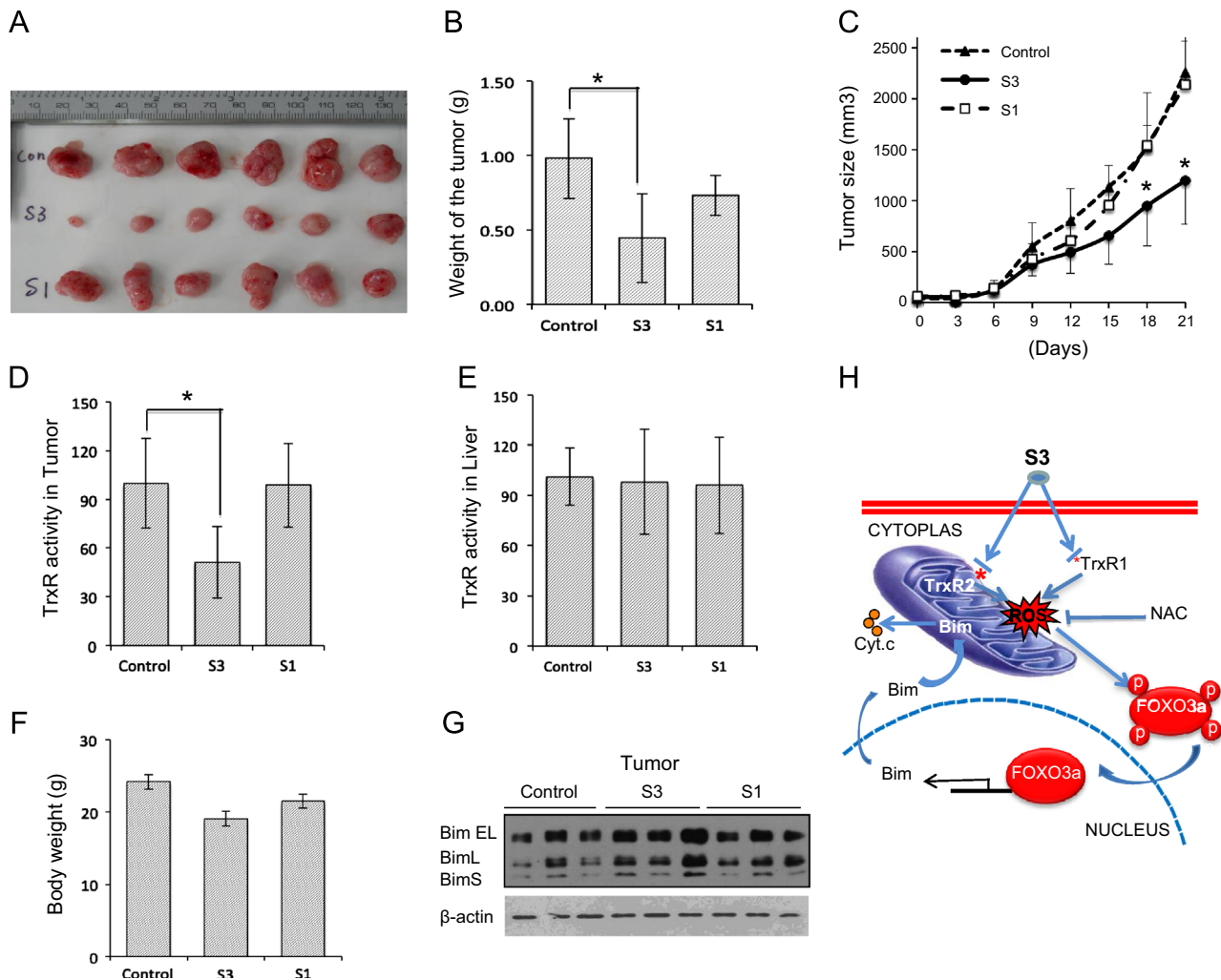
Fig. 6. S3 inhibits tumor growth in vivo by inhibiting TrxR activity in mice. (A) Image of representative tumors of the control groups and the S3- and S1-treated groups. (B) The mean mass of the tumors from the three groups at the end of treatment with SD indicated by the error bars. (C) The tumor growth curve in the treatment within 3 weeks. (D and E) The statistical results of TrxR activity were measured in tumors (D) and liver tissues (E). (F) The body weight of mice from the three groups at the end of treatment. (G) Western blotting analysis of Bim expression in three respresentative tumors from each of the three groups at the end of treatment. The data are representative of the mean value of at least three separate experiments, and statistical significance was determined using Student's t test. *$P < 0.05$ compared with the control group. (H) The model of S3 targets TrxR1 and TrxR2 for Bim upregulation (*Indicates the selenocysteine in TrxR).

retarded tumor growth via inhibition of TrxR to overcome drug resistance in the absence of Bax and Bak.

Discussion

Our previously study found that S3 induces Bax/Bak-independent apoptosis through the upregulation of Bim, which interacts with Bcl-2 to permeabilize the mitochondrial outer membrane for cytochrome *c* release and apoptosis [45]. To detect the mechanism of Bim upregulation, we used a chemical biology approach to identify possible targets of S3 and our results showed that S3 forms a covalent complex with TrxR in the selenocysteine residue to inhibit activity (Fig. 1D and E; Fig. 2A and C), resulting in perturbing the redox system in the cytoplasm and within mitochondria. This change leads to the ample production of ROS for the activation of FOXO3, which transcriptionally upregulates Bim to promote apoptosis (Fig. 3A, Figs. 5A–C, E, 6H). However, S1, the "loss of function" precursor of S3, neither inhibits TrxR activity nor attenuates apoptosis (Figs. 2A and 3D). These results directly link the inactivation of TrxR activity to the cell death.

We found that inhibition of mammalian TrxR by S3 is achieved through specific targeting of the C-terminal active-site

residues (Sec) (Fig. 2D and E). S3 shows a strong inhibitory effect on isolated wild-type mammalian TrxR with lower IC_{50} values (Fig. 2C). TrxR mutants lacking the selenocysteine, as well as GR (lacks selenocysteine in the reactive center), are comparatively insensitive to S3 treatment (Fig. 2B and D). Based on our results, we proposed that S3 directly attacks the selenolate moiety of NADPH-reduced TrxR. As a result, the reactive Sec498 of TrxR is chemically modified by S3 to lose catalytic activity. The inhibitory properties of S3 on mammalian TrxR are comparable with those of some metal-based compounds and alkylating agents that have been reported as TrxR inhibitors [22]. It is a common feature that inhibition of TrxR by these agents causes ROS production and oxidative stress [9,57]. As S3, but not S1, has a carbonyl group that is reactive to redox-sensitive cysteine, it is possible that there might be other molecular targets participating in the induction of apoptosis by S3. Indeed, previous study showed that S3 targets the Wnt pathway to inhibit anchorage-independent growth and xenograft tumorigenesis of SW480 cells *in vivo* [58].

The TrxR system is an essential redox regulator in many cell physiology functions. Recently, augmentation of the expression and transcription level of TrxRs, leading to increased TrxR protein and activity levels, is found in different kinds of human tumor cells

[33,59]. All these results indicated that TrxR is extremely important for cancer cell survival and propagation. Considering the important functions of TrxRs in cancer development and progression, TrxRs are now major targets for anticancer drugs. Previous reports have shown that the targeting of TrxR with electrophiles leads to Bax/Bak-dependent apoptosis [60]. It has been suggested that this occurrence may result in oxidative stress and p53 activation, which transcriptionally increases Bax or puma expression responsible for apoptosis [61,62]. ROS may directly react with the conserved cysteine residues and activate Bax for apoptosis, as we showed previously [63]. The current study specifically addresses how TrxR inhibition leads to Bax- and Bak-independent apoptosis. Our results showed that inhibition resulted in pronounced ROS production for subsequent FoxO3 activation, which is responsible for Bim induction [55,64,65]. Inhibition of TrxR also modulates redox-sensitive signaling molecules such as JNK and ERK that lead to the activation of FoxO3 (unpublished observation). Both TrxR and Trx are involved in many apoptosis modulation pathways, such as P53 [23,36], ASK1 activation [37], and NF-κB activation [8], further experiments are also needed to clarify the other mechanism of S3-induced apoptosis. It is conceivable that the dysregulation of Bcl-2 family proteins and an increase in TrxR expression were found in many types of cancers [32,59,66], so both inhibition of TrxR and activation of Bcl-2 family protein-dependent apoptosis by a single agent provide a powerful strategy for therapeutic application in fighting cancers [67].

Acknowledgments

Appendix A. Supporting information

Supplementary data associated with this article can be found in the online version at http://dx.doi.org/10.1016/j.freeradbiomed.2013.05.038.

References

[1] Powis, G.; Gasdaska, J. R.; Gasdaska, P. Y.; Berggren, M.; Kirkpatrick, D. L.; Engman, L.; Cotgreave, I. A.; Angulo, M.; Baker, A. Selenium and the thioredoxin redox system: effects on cell growth and death. *Oncol. Res.* **9:**303–312; 1997.

[2] Sun, Y.; Rigas, B. The thioredoxin system mediates redox-induced cell death in human colon cancer cells: implications for the mechanism of action of anticancer agents. *Cancer Res* **68:**8269–8277; 2008.

[3] Zhang, X.; Zheng, Y.; Fried, L. E.; Du, Y.; Montano, S. J.; Sohn, A.; Lefkove, B.; Holmgren, L.; Arbiser, J. L.; Holmgren, A.; Lu, J. Disruption of the mitochondrial thioredoxin system as a cell death mechanism of cationic triphenylmethanes. *Free Radic. Biol. Med.* **50:**811–820; 2011.

[4] Yin, F.; Sancheti, H.; Cadenas, E. Mitochondrial thiols in the regulation of cell death pathways. *Antioxid. Redox Signal.* **17:**1714–1727; 2012.

[5] Das, K. C. Thioredoxin system in premature and newborn biology. *Antioxid. Redox Signal.* **6:**177–184; 2004.

[6] Patenaude, A.; Ven Murthy, M. R.; Mirault, M. E. Mitochondrial thioredoxin system: effects of TrxR2 overexpression on redox balance, cell growth, and apoptosis. *J. Biol. Chem.* **279:**27302–27314; 2004.

[7] Zhao, F.; Yan, J.; Deng, S.; Lan, L.; He, F.; Kuang, B.; Zeng, H. A thioredoxin reductase inhibitor induces growth inhibition and apoptosis in five cultured human carcinoma cell lines. *Cancer Lett.* **236:**46–53; 2006.

[8] Lan, L.; Zhao, F.; Wang, Y.; Zeng, H. The mechanism of apoptosis induced by a novel thioredoxin reductase inhibitor in A549 cells: possible involvement of nuclear factor-kappaB-dependent pathway. *Eur. J. Pharmacol* **555:**83–92; 2007.

[9] Yan, C.; Siegel, D.; Newsome, J.; Chilloux, A.; Moody, C. J.; Ross, D. Antitumor indolequinones induced apoptosis in human pancreatic cancer cells via inhibition of thioredoxin reductase and activation of redox signaling. *Mol. Pharmacol.* **81:**401–410; 2012.

[10] Luthman, M.; Holmgren, A. Rat liver thioredoxin and thioredoxin reductase: purification and characterization. *Biochemistry* **21:**6628–6633; 1982.

[11] Lee, S. R.; Kim, J. R.; Kwon, K. S.; Yoon, H. W.; Levine, R. L.; Ginsburg, A.; Rhee, S. G. Molecular cloning and characterization of a mitochondrial selenocysteine-containing thioredoxin reductase from rat liver. *J. Biol. Chem.* **274:**4722–4734; 1999.

[12] Miranda-Vizuete, A.; Damdimopoulos, A. E.; Pedrajas, J. R.; Gustafsson, J. A.; Spyrou, G. Human mitochondrial thioredoxin reductase cDNA cloning, expression and genomic organization. *Eur. J. Biochem./ FEBS* **261:**405–412; 1999.

[13] Kryukov, G. V.; Castellano, S.; Novoselov, S. V.; Lobanov, A. V.; Zehtab, O.; Guigo, R.; Gladyshev, V. N. Characterization of mammalian selenoproteomes. *Science* **300:**1439–1443; 2003.

[14] Arner, E. S.; Nordberg, J.; Holmgren, A. Efficient reduction of lipoamide and lipoic acid by mammalian thioredoxin reductase. *Biochem. Biophys. Res. Commun.* **225:**268–274; 1996.

[15] Turanov, A. A.; Hatfield, D. L.; Gladyshev, V. N. Characterization of protein targets of mammalian thioredoxin reductases. *Methods Enzymol.* **474:**245–254; 2010.

[16] Lee, S. R.; Bar-Noy, S.; Kwon, J.; Levine, R. L.; Stadtman, T. C.; Rhee, S. G. Mammalian thioredoxin reductase: oxidation of the C-terminal cysteine/selenocysteine active site forms a thioselenide, and replacement of selenium with sulfur markedly reduces catalytic activity. *Proc. Natl. Acad. Sci. USA* **97:**2521–2526; 2000.

[17] Biterova, E. I.; Turanov, A. A.; Gladyshev, V. N.; Barycki, J. J. Crystal structures of oxidized and reduced mitochondrial thioredoxin reductase provide molecular details of the reaction mechanism. *Proc. Natl. Acad. Sci. USA* **102:**15018–15023; 2005.

[18] Fritz-Wolf, K.; Urig, S.; Becker, K. The structure of human thioredoxin reductase 1 provides insights into C-terminal rearrangements during catalysis. *J. Mol. Biol* **370:**116–127; 2007.

[19] Zhong, L.; Holmgren, A. Essential role of selenium in the catalytic activities of mammalian thioredoxin reductase revealed by characterization of recombinant enzymes with selenocysteine mutations. *J. Biol. Chem* **275:**18121–18128; 2000.

[20] Selenius, M.; Rundlof, A. K.; Olm, E.; Fernandes, A. P.; Bjornstedt, M. Selenium and the selenoprotein thioredoxin reductase in the prevention, treatment and diagnostics of cancer. *Antioxid. Redox Signal.* **12:**867–880; 2010.

[21] Karimpour, S.; Lou, J.; Lin, L. L.; Rene, L. M.; Lagunas, L.; Ma, X.; Karra, S.; Bradbury, C. M.; Markovina, S.; Goswami, P. C.; Spitz, D. R.; Hirota, K.; Kalvakolanu, D. V.; Yodoi, J.; Gius, D. Thioredoxin reductase regulates AP-1 activity as well as thioredoxin nuclear localization via active cysteines in response to ionizing radiation. *Oncogene* **21:**6317–6327; 2002.

[22] Fang, J.; Lu, J.; Holmgren, A. Thioredoxin reductase is irreversibly modified by curcumin: a novel molecular mechanism for its anticancer activity. *J. Biol. Chem.* **280:**25284–25290; 2005.

[23] Hu, J.; Ma, X.; Lindner, D. J.; Karra, S.; Hofmann, E. R.; Reddy, S. P.; Kalvakolanu, D. V. Modulation of p53 dependent gene expression and cell death through thioredoxin-thioredoxin reductase by the interferon-retinoid combination. *Oncogene* **20:**4235–4248; 2001.

[24] Sohn, K. C.; Jang, S.; Choi, D. K.; Lee, Y. S.; Yoon, T. J.; Jeon, E. K.; Kim, K. H.; Seo, Y. J.; Lee, J. H.; Park, J. K.; Kim, C. D. Effect of thioredoxin reductase 1 on glucocorticoid receptor activity in human outer root sheath cells. *Biochem. Biophys. Res. Commun.* **356:**810–815; 2007.

[25] Zhou, J.; Eleni, C.; Spyrou, G.; Brune, B. The mitochondrial thioredoxin system regulates nitric oxide-induced HIF-1alpha protein. *Free Radic. Biol. Med.* **44:**91–98; 2008.

[26] Naranjo-Suarez, S.; Carlson, B. A.; Tsuji, P. A.; Yoo, M. H.; Gladyshev, V. N.; Hatfield, D. L. HIF-independent regulation of thioredoxin reductase 1 contributes to the high levels of reactive oxygen species induced by hypoxia. *PloS One* **7:**e30470; 2012.

[27] Conrad, M.; Jakupoglu, C.; Moreno, S. G.; Lippl, S.; Banjac, A.; Schneider, M.; Beck, H.; Hatzopoulos, A. K.; Just, U.; Sinowatz, F.; Schmahl, W.; Chien, K. R.; Wurst, W.; Bornkamm, G. W.; Brielmeier, M. Essential role for mitochondrial thioredoxin reductase in hematopoiesis, heart development, and heart function. *Mol. Cell. Biol.* **24:**9414–9423; 2004.

[28] Jakupoglu, C.; Przemeck, G. K.; Schneider, M.; Moreno, S. G.; Mayr, N.; Hatzopoulos, A. K.; de Angelis, M. H.; Wurst, W.; Bornkamm, G. W.; Brielmeier, M.; Conrad, M. Cytoplasmic thioredoxin reductase is essential for embryogenesis but dispensable for cardiac development. *Mol. Cell. Biol.* **25:**1980–1988; 2005.

[29] Bondareva, A. A.; Capecchi, M. R.; Iverson, S. V.; Li, Y.; Lopez, N. I.; Lucas, O.; Merrill, G. F.; Prigge, J. R.; Siders, A. M.; Wakamiya, M.; Wallin, S. L.; Schmidt, E. E. Effects of thioredoxin reductase-1 deletion on embryogenesis and transcriptome. *Free Radic. Biol. Med.* **43:**911–923; 2007.

[30] Kakolyris, S.; Giatromanolaki, A.; Koukourakis, M.; Powis, G.; Souglakos, J.; Sivridis, E.; Georgoulias, V.; Gatter, K. C.; Harris, A. L. Thioredoxin expression is associated with lymph node status and prognosis in early operable non-small cell lung cancer. *Clin. Cancer Res.* **7:**3087–3091; 2001.

[31] Engman, L.; Al-Maharik, N.; McNaughton, M.; Birmingham, A.; Powis, G. Thioredoxin reductase and cancer cell growth inhibition by organotellurium antioxidants. *Anti-cancer drugs* **14:**153–161; 2003.

[32] Lincoln, D. T.; Ali Emadi, E. M.; Tonissen, K. F.; Clarke, F. M. The thioredoxin-thioredoxin reductase system: over-expression in human cancer. *Anticancer Res.* **23:**2425–2433; 2003.

[33] Raffel, J.; Bhattacharyya, A. K.; Gallegos, A.; Cui, H.; Einspahr, J. G.; Alberts, D. S.; Powis, G. Increased expression of thioredoxin-1 in human colorectal cancer is associated with decreased patient survival. *J. Lab. Clin. Med.* **142:**46–51; 2003.

[34] Biaglow, J. E.; Miller, R. A. The thioredoxin reductase/thioredoxin system: novel redox targets for cancer therapy. *Cancer Biol. Ther.* **4:**6–13; 2005.

[35] Nguyen, P.; Awwad, R. T.; Smart, D. D.; Spitz, D. R.; Gius, D. Thioredoxin reductase as a novel molecular target for cancer therapy. *Cancer Lett.* **236:**164–174; 2006.

[36] Moos, P. J.; Edes, K.; Cassidy, P.; Massuda, E.; Fitzpatrick, F. A. Electrophilic prostaglandins and lipid aldehydes repress redox-sensitive transcription factors p53 and hypoxia-inducible factor by impairing the selenoprotein thioredoxin reductase. *J. Biol. Chem.* **278:**745–750; 2003.

[37] Saitoh, M.; Nishitoh, H.; Fujii, M.; Takeda, K.; Tobiume, K.; Sawada, Y.; Kawabata, M.; Miyazono, K.; Ichijo, H. Mammalian thioredoxin is a direct inhibitor of apoptosis signal-regulating kinase (ASK) 1. *EMBO J.* **17:**2596–2606; 1998.

[38] Ueda, S.; Masutani, H.; Nakamura, H.; Tanaka, T.; Ueno, M.; Yodoi, J. Redox control of cell death. *Antioxid. Redox Signal.* **4:**405–414; 2002.

[39] Liu, C.; Liu, Z.; Li, M.; Li, X.; Wong, Y. S.; Ngai, S. M.; Zheng, W.; Zhang, Y.; Chen, T. Enhancement of auranofin-induced apoptosis in mcf-7 human breast cells by selenocystine, a synergistic inhibitor of thioredoxin reductase. *PloS One* : e53945; 2013.

[40] Degenhardt, K.; Chen, G.; Lindsten, T.; White, E.; BAX, B. A. K. mediate p53-independent suppression of tumorigenesis. *Cancer Cell* **2:**193–203; 2002.

[41] Yin, C.; Knudson, C. M.; Korsmeyer, S. J.; Van Dyke, T. Bax suppresses tumorigenesis and stimulates apoptosis in vivo. *Nature* **385:**637–640; 1997.

[42] Mrozek, A.; Petrowsky, H.; Sturm, I.; Kraus, J.; Hermann, S.; Hauptmann, S.; Lorenz, M.; Dorken, B.; Daniel, P. T. Combined p53/Bax mutation results in extremely poor prognosis in gastric carcinoma with low microsatellite instability. *Cell Death Differ.* **10:**461–467; 2003.

[43] Thomas, A.; El Rouby, S.; Reed, J. C.; Krajewski, S.; Silber, R.; Potmesil, M.; Newcomb, E. W. Drug-induced apoptosis in B-cell chronic lymphocytic leukemia: relationship between p53 gene mutation and bcl-2/bax proteins in drug resistance. *Oncogene* **12:**1055–1062; 1996.

[44] Kim, M. S.; Kim, S. S.; Yoo, N. J.; Lee, S. H. Rare somatic mutation of pro-apoptotic BAX and BAK genes in common human cancers. *Tumori* **98:**149e–151e; 2012.

[45] Zhao, L.; He, F.; Liu, H.; Zhu, Y.; Tian, W.; Gao, P.; He, H.; Yue, W.; Lei, X.; Ni, B.; Wang, X.; Jin, H.; Hao, X.; Lin, J.; Chen, Q. Natural diterpenoid compound elevates expression of Bim protein, which interacts with antiapoptotic protein Bcl-2, converting it to proapoptotic Bax-like molecule. *J. Biol. Chem.* **287:**1054–1065; 2012.

[46] Smith, D. B.; Johnson, K. S. Single-step purification of polypeptides expressed in Escherichia coli as fusions with glutathione S-transferase. *Gene* **67:**31–40; 1988.

[47] Liu, C. X.; Yin, Q. Q.; Zhou, H. C.; Wu, Y. L.; Pu, J. X.; Xia, L.; Liu, W.; Huang, X.; Jiang, T.; Wu, M. X.; He, L. C.; Zhao, Y. X.; Wang, X. L.; Xiao, W. L.; Chen, H. Z.; Zhao, Q.; Zhou, A. W.; Wang, L. S.; Sun, H. D.; Chen, G. Q. Adenanthin targets peroxiredoxin I and II to induce differentiation of leukemic cells. *Nat. Chem. Biol.* **8:**486–493; 2012.

[48] Gierse, J. K.; Koboldt, C. M.; Walker, M. C.; Seibert, K.; Isakson, P. C. Kinetic basis for selective inhibition of cyclo-oxygenases. *Biochem. J.* **339:**607–614; 1999. **Pt 3**.

[49] Ahn, K.; Johnson, D. S.; Mileni, M.; Beidler, D.; Long, J. Z.; McKinney, M. K.; Weerapana, E.; Sadagopan, N.; Liimatta, M.; Smith, S. E.; Lazerwith, S.; Stiff, C.;

Kamtekar, R. C.; Bhattacharya, K.; Zhang, Y.; Swaney, S.; Van Becelaere, K.; Stevens, R. C.; Cravatt, B. F. Discovery and characterization of a highly selective FAAH inhibitor that reduces inflammatory pain. *Chem. Biol.* **16:**411–420; 2009.

[50] Anestal, K.; Prast-Nielsen, S.; Cenas, N.; Arner, E. S. Cell death by SecTRAPs: thioredoxin reductase as a prooxidant killer of cells. *PloS One* **3:**e1846; 2008.

[51] Nordberg, J.; Arner, E. S. Reactive oxygen species, antioxidants, and the mammalian thioredoxin system. *Free Radic. Biol. Med.* **31:**1287–1312; 2001.

[52] Arner, E. S.; Bjornstedt, M.; Holmgren, A. 1-Chloro-2,4-dinitrobenzene is an irreversible inhibitor of human thioredoxin reductase. Loss of thioredoxin disulfide reductase activity is accompanied by a large increase in NADPH oxidase activity. *J. Biol. Chem* **270:**3479–3482; 1995.

[53] Brunet, A.; Bonni, A.; Zigmond, M. J.; Lin, M. Z.; Juo, P.; Hu, L. S.; Anderson, M. J.; Arden, K. C.; Blenis, J.; Greenberg, M. E. Akt promotes cell survival by phosphorylating and inhibiting a Forkhead transcription factor. *Cell* **96:**857–868; 1999.

[54] Dijkers, P. F.; Medema, R. H.; Lammers, J. W.; Koenderman, L.; Coffer, P. J. Expression of the pro-apoptotic Bcl-2 family member Bim is regulated by the forkhead transcription factor FKHR-L1. *Curr. Biol.* **10:**1201–1204; 2000.

[55] Urbich, C.; Knau, A.; Fichtlscherer, S.; Walter, D. H.; Bruhl, T.; Potente, M.; Hofmann, W. K.; de Vos, S.; Zeiher, A. M.; Dimmeler, S. FOXO-dependent expression of the proapoptotic protein Bim: pivotal role for apoptosis signaling in endothelial progenitor cells. *FASEB J* **19:**974–976; 2005.

[56] Ni, B.; Ma, Q.; Li, B.; Zhao, L.; Liu, Y.; Zhu, Y.; Chen, Q. Phenylarsine oxide induces apoptosis in Bax- and Bak-deficient cells through upregulation of Bim. *Clin. Cancer Res.* **18:**140–151; 2012.

[57] Liu, J. J.; Liu, Q.; Wei, H. L.; Yi, J.; Zhao, H. S.; Gao, L. P. Inhibition of thioredoxin reductase by auranofin induces apoptosis in adriamycin-resistant human K562 chronic myeloid leukemia cells. *Pharmazie* **66:**440–444; 2011.

[58] Wang, W.; Liu, H.; Wang, S.; Hao, X.; Li, L. A diterpenoid derivative 15-oxospiramilactone inhibits Wnt/beta-catenin signaling and colon cancer cell tumorigenesis. *Cell Res.* **21:**730–740; 2011.

[59] Kim, S. J.; Miyoshi, Y.; Taguchi, T.; Tamaki, Y.; Nakamura, H.; Yodoi, J.; Kato, K.; Noguchi, S. High thioredoxin expression is associated with resistance to docetaxel in primary breast cancer. *Clin. Cancer Res.* **11:**8425–8430; 2005.

[60] Cox, A. G.; Brown, K. K.; Arner, E. S.; Hampton, M. B. The thioredoxin reductase inhibitor auranofin triggers apoptosis through a Bax/Bak-dependent process that involves peroxiredoxin 3 oxidation. *Biochem. Pharmacol.* **76:**1097–1109; 2008.

[61] Skirnisdottir, I.; Seidal, T. The apoptosis regulators p53, bax and PUMA: Relationship and impact on outcome in early stage (FIGO I-II) ovarian carcinoma after post-surgical taxane-based treatment. *Oncol. Rep* **27:**741–747; 2012.

[62] Sinha, S.; Malonia, S. K.; Mittal, S. P.; Singh, K.; Kadreppa, S.; Kamat, R.; Mukhopadhyaya, R.; Pal, J. K.; Chattopadhyay, S. Coordinated regulation of p53 apoptotic targets BAX and PUMA by SMAR1 through an identical MAR element. *EMBO J.* **29:**830–842; 2010.

[63] Nie, C.; Tian, C.; Zhao, L.; Petit, P. X.; Mehrpour, M.; Chen, Q. Cysteine 62 of Bax is critical for its conformational activation and its proapoptotic activity in response to H$_2$O$_2$-induced apoptosis. *J. Biol. Chem.* **283:**15359–15369; 2008.

[64] Gilley, J.; Coffer, P. J.; Ham, J. FOXO transcription factors directly activate bim gene expression and promote apoptosis in sympathetic neurons. *J. Cell Biol.* **162:**613–622; 2003.

[65] Sunters, A.; Fernandez de Mattos, S.; Stahl, M.; Brosens, J. J.; Zoumpoulidou, G.; Saunders, C. A.; Coffer, P. J.; Medema, R. H.; Coombes, R. C.; Lam, E. W. *FoxO3a transcriptional regulation of Bim controls apoptosis in paclitaxel-treated breast cancer cell lines. J. Biol. Chem.*, **278**; 49795–49805; 2003.

[66] Goldsmith, K. C.; Gross, M.; Peirce, S.; Luyindula, D.; Liu, X.; Vu, A.; Sliozberg, M.; Guo, R.; Zhao, H.; Reynolds, C. P.; Hogarty, M. D. Mitochondrial Bcl-2 family dynamics define therapy response and resistance in neuroblastoma. *Cancer Res.* **72:**2565–2577; 2012.

[67] Wondrak, G. T. Redox-directed cancer therapeutics: molecular mechanisms and opportunities. *Antioxid. Redox Signal.* **11:**3013–3069; 2009.